Inorganic Chemistry
COMMUNICATION
pubs.acs.org/IC

Surface Activation of Electrocatalysis at Oxide Electrodes. Concerted Electron−Proton Transfer

Christopher J. Gagliardi, Jonah W. Jurss, H. Holden Thorp, and Thomas J. Meyer*

Department of Chemistry, University of North Carolina at Chapel Hill, Chapel Hill, North Carolina 27599-3290, United States

S *Supporting Information*

ABSTRACT: Dramatic rate enhancements are observed for the oxidation of phenols, including tyrosine, at indium−tin oxide electrodes modified by the addition of the electron-transfer relays $[M^{II}(bpy)_2(4,4'\text{-}(HO)_2P(O)CH_2)_2bpy)]^{2+}$ (M = Ru, Os) with clear evidence for the importance of proton-coupled electron transfer and concerted electron−proton transfer.

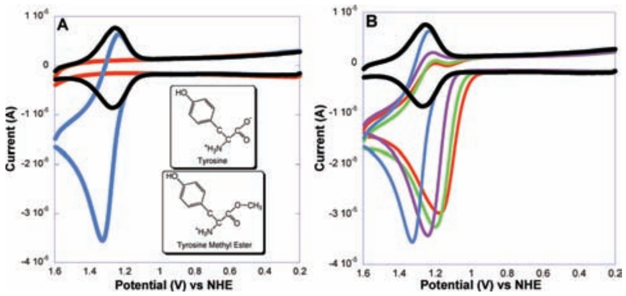

Figure 1. (A) Cyclic voltammograms of TyrOH (0.1 mM) in 0.1 M $HClO_4$/0.8 M in $LiClO_4$ at 300 mV/s, at ITO (red), at **ITO-Ru^{II}** ($\Gamma = 1.2 \times 10^{-10}$ mol/cm^2, black, see text) and at **ITO-Ru^{II}** + TyrOH at 25 ± 2 °C (blue). (B) As in part A, in 0.1 M $HClO_4$/0.8 M $LiClO_4$ (blue) and in 50 mM buffers, 4.55 mM in buffer base at a 10:1 acid/base buffer ratio of acetate (purple, $HOAc/OAc^-$, pK_a 4.7 at pH 3.7), citrate (green, $H_3C_6H_5O_7/H_2C_6H_5O_7^-$, p$K_a$ 6.4 at pH 5.4), phosphate (red, $H_2PO_4^-/HPO_4^{2-}$, pK_a 7.2 at pH 6.2), and **ITO-Ru^{II}** (black).

Conducting oxide electrodes such as ITO, tin-doped In_2O_3 (In_2O_3:Sn), and FTO, fluorine-doped SnO_2, are commonly used in electrochemistry. For reversible couples in nonaqueous solvents, ITO and FTO behave similarly to typical metal or carbon electrodes. However, for small organic molecules in aqueous solution, there is often no electrochemical response within the solvent limit. This effect has been exploited, for example, in the study of amino acid oxidation by diffusional couples such as $Ru(bpy)_3^{3+/2+}$.[1,2] The absence of facile electrochemistry at these electrodes considerably limits their application in analytical and electrocatalytic applications.[1−3]

In an earlier study, we reported surface catalysis of water oxidation at ITO derivatized by surface binding of the electron-transfer relay $[Ru^{II}(bpy)(4,4'\text{-}(HO)_2P(O)CH_2)_2bpy)_2]^{2+}$ [bpy = 2,2′ - bipyridine; $4,4'\text{-}(HO)_2P(O)CH_2)_2$bpy = 4,4′-bis(methylenephosphonato)-2,2′-bipyridine].[4] Here we report dramatic rate enhancements for the oxidation of tyrosine (TyrOH) and tyrosine methyl ester, whose structures are shown as insets in Figure 1A, and 4-methylphenol (4-MeArOH) at ITO electrodes modified by surface-attached $[Ru^{II}(bpy)_2(4,4'\text{-}(HO)_2P(O)CH_2)_2bpy)]^{2+}$ (**ITO-Ru^{II}**) and ITO-bound $[Os^{II}(bpy)_2(4,4'\text{-}(HO)_2P(O)CH_2)_2bpy)]^{2+}$ (**ITO-Os^{II}**). We also provide clear evidence for an important role for proton-coupled electron transfer (PCET) and concerted electron-proton transfer (EPT) pathways at these chemically modified interfaces.

Surface phosphonate binding to oxide electrodes including ITO, FTO, and nanostructured TiO_2 is well documented.[5,6] We prepared **ITO-Ru^{II}** and **ITO-Os^{II}** by soaking slides in solutions containing 1×10^{-4} M complex in 0.1 M HNO_3 or $HClO_4$ for 4 h followed by rinsing with methanol.[4] Different surface loadings were studied by soaking slides in solutions containing lower concentrations of the complex. The surface coverage was determined by cyclic voltammetry by peak current measurements (see the Supporting Information, SI), as described previously.[7]

The electrochemistry of phenols, including the role of PCET, has been studied in detail by Savéant and co-workers at glassy carbon electrodes.[3] As shown in Figures 1 and SI1 in the SI, at ITO there is no electrochemical response with the amino acid tyrosine added to the background limit at ∼1.6 V vs NHE from pH 1 to 8.

Surface modification results in dramatic changes in the electrochemical response for all three phenols. At **ITO-Ru^{II}** in water, a reversible surface wave appears for the ITO-Ru$^{III/II}$ couple at 1.25 V vs normal hydrogen electrode(NHE). With added TyrOH in 0.1 M $HClO_4$/0.8 M $LiClO_4$, an additional, irreversible wave appears for the pH-dependent $TyrO^\bullet$/TyrOH couple at E_p = 1.33 V vs NHE.[3] As shown in Figure SI2 in the SI, the peak current (i_p) varies with the scan rate (ν) for the ITO-Ru$^{III/II}$ surface couple and with $\nu^{1/2}$ for the $TyrO^\bullet$/TyrOH couple, as predicted for surface and diffusional couples, respectively.[8] Similar results were obtained for both the ester and phenol.

Peak currents for the TyrOH oxidation wave, i_p, vary linearly with [TyrOH] (50−150 μM) and linearly with Ru^{II} surface coverage from $\Gamma/\Gamma_0 = 1$ (monolayer surface coverage: $\Gamma_0 = 1.2 \times 10^{-10}$ mol/cm^2) to 4.2×10^{-11} mol/cm^2 ($\Gamma/\Gamma_0 = 0.35$); see Figure SI3 in the SI. The peak potential at pH 1 (1.33 V) is consistent with $E^{\circ\prime} \approx 1.5$ V for the $TyrOH^{\bullet+}$/TyrOH couple and pK_a = −2 for $TyrOH^{\bullet+}$.[9,10]

The experimental observations are consistent with the surface activation of electron transfer by the mechanism shown in Scheme 1.[11] In this mechanism, rapid surface oxidation of **ITO-Ru^{II}** to **ITO-Ru^{III}** is followed by rate-limiting interfacial oxidation of TyrOH to $TyrOH^{\bullet+}$ by electron transfer.[12−14] The

Received: December 17, 2010
Published: February 08, 2011

dx.doi.org/10.1021/ic102524f | *Inorg. Chem.* 2011, 50, 2076–2078

Scheme 1

$$\begin{aligned}
\text{ITO-Ru}^{2+} &\overset{e^-}{\rightleftharpoons} \text{ITO-Ru}^{3+}\\
\text{ITO-Ru}^{3+} + \text{TyrOH} &\rightleftharpoons \text{ITO-Ru}^{3+}\text{,TyrOH: } K_A\\
\text{ITO-Ru}^{3+}\text{,TyrOH} &\longrightarrow \text{ITO-Ru}^{2+} + \text{TyrOH}^{+\bullet}\text{: } k_{ET}\\
2\text{TyrOH}^{+\bullet} &\longrightarrow (\text{TyrO})_2 + 2\text{H}^+
\end{aligned}$$

surface ITO-Ru$^{III/II}$ couple is electrochemically reversible over a wide range of scan rates; the rate constant for Ru(bpy)$_3{}^{3+/2+}$ self-exchange in solution is ~10^8 M^{-1} s^{-1}.[15]

A rate constant for the surface oxidation of TyrOH was obtained by peak current measurements and the expression $i_{cat} = nFAk_{cat}\Gamma[\text{TyrOH}]$, with i_{cat} the catalytic current, n the number of electrons transferred (assumed to be 1), A the surface area, Γ the surface coverage of **ITO-Ru^{II}** in mol/cm^2, and k_{cat} the surface catalytic rate constant.[16] As shown by the plot of $i_{cat}/nFA\Gamma$ vs [TyrOH] in Figure SI4 in the SI, k_{cat} varies with [TyrOH], and from the slope, $k = 8.0 \times 10^4$ M^{-1} s^{-1} at 25 ± 2 °C in 0.1 M HClO$_4$ and 0.8 M LiClO$_4$. For the solution oxidation of TyrOH by Ru(bpy)$_3{}^{3+}$ under comparable conditions, $k = K_Ak_{ET} = 3.0 \times 10^5$ M^{-1} s^{-1}.[1,2]

In contrast to phenol oxidation at glassy carbon,[3] the H$_2$O/D$_2$O kinetic isotope (KIE) is small with $k(\text{H}_2\text{O})/k(\text{D}_2\text{O}) \sim 1.2$, consistent with electron transfer as the dominant redox step at the electrode rather than concerted EPT with proton transfer to the solvent.

As shown in Figures 1B and SI5 in the SI, there is evidence for an additional catalytic effect with added acetate (10:1 HOAc/OAc$^-$ at pH 3.7), citrate (10:1 H$_3$C$_6$H$_5$O$_7$/H$_2$C$_6$H$_5$O$_7{}^-$ at pH 5.4), and phosphate (10:1 H$_2$PO$_4{}^-$/HPO$_4{}^{2-}$ at pH 6.2) buffers. At high limiting buffer base concentrations, 4.5 mM, and a scan rate of 300 mV/s, E_p shifts to 1.24, 1.20, and 1.18 V, respectively. This is a buffer base effect and not a pH effect. As noted in Figure SI6 in the SI for the HOAc/OAc$^-$ buffer, E_p is virtually unaffected by pH changes from 3.8 to 5.8 at [OAc$^-$] = 4.5 mM. In solutions diluted in a citrate buffer (pH 5.4, 0.01 mM), there is no buffer effect with E_p = 1.24 V (Figure SI7 in the SI), the same value as that in 10^{-3} M HClO$_4$.[17,18]

The trend in E_p values in Figure 1B follows the base strengths of the buffer bases with pK_a(HB) = 4.7, 6.4, and 7.2 for acetate, citrate, and HPO$_4{}^{2-}$, respectively. They are more positive than $E°'$ values for the pH-dependent TyrO$^\bullet$/TyrOH couple with $E°'$ = 1.06 (pH 3.7), 0.96 (pH 5.4), and 0.92 (pH 6.2) V. These values were calculated from $E°'$(TyrOH$^{\bullet+}$/TyrOH) = 1.46 V and pK_a(TyrOH$^{\bullet+}$) = −2 (eq SI1 in the SI).[19,20]

Quantitative simulations of the cyclic voltammograms are not yet available, but the base effect is qualitatively consistent with the mechanism in Scheme 2. In this scheme, preassociation occurs with the buffer base to give the hydrogen-bonded adduct, TyrOH---B. It is followed by concerted, multisite electron−proton transfer (MS-EPT) at the electrode with electron transfer to **ITO-Ru^{III}** and proton transfer to B (Figure 2). A related pathway has been identified in the oxidation of TyrOH by M(bpy)$_3{}^{3+}$ (M = Fe, Ru, Os) in solution.[1,2]

As calculated from the expression $E_{1/2}(\text{calc}) \sim E_{1/2}(\text{TyrOH}^{\bullet+/0}) + 0.059\{\text{p}K_a(\text{TyrOH}^{\bullet+}) - \text{p}K_a(\text{HB})\}$, the $E°'$ values for the adduct couples in Scheme 2, TyrOH---B/TyrO$^\bullet$---$^+$H−B, are more positive than expected. For example, E_p = 1.24 V for OAc$^-$, while $E_{1/2}$(calc) = 1.06 V.[21] The waves are also scan-rate-dependent, with E_p shifting to more negative potentials as the scan rate is decreased and i_p decreasing as E_p decreases (Figure SI8 in the SI). These observations are qualitatively consistent with the surface EPT rate limited by the low surface concentration of **ITO-Ru^{III}** at the potentials at which oxidation occurs. For the surface couple, $E_{1/2}$(ITO-Ru$^{III/II}$) = 1.25 V.

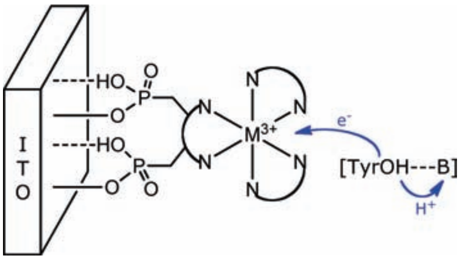

Figure 2. Illustration of surface MS-EPT with electron transfer to ITO-Ru^{3+} and proton transfer to an added buffer base, B, as the proton acceptor.

Scheme 2

$$\begin{aligned}
\text{TyrOH} + \text{B} &\rightleftharpoons \text{TyrOH--B: } K_A\\
\text{ITO-Ru}^{2+} &\overset{e^-}{\rightleftharpoons} \text{ITO-Ru}^{3+}\\
\text{ITO-Ru}^{3+} + \text{TyrOH--B} &\rightleftharpoons \text{ITO-Ru}^{3+}\text{,TyrOH--B: } K_A'\\
\text{ITO-Ru}^{3+}\text{,TyrOH--B} &\longrightarrow \text{ITO-Ru}^{2+} + \text{TyrO}^\bullet + {}^+\text{HB: } k_{EPT}\\
2\text{TyrO}^\bullet &\longrightarrow (\text{TyrO})_2
\end{aligned}$$

Scheme 3

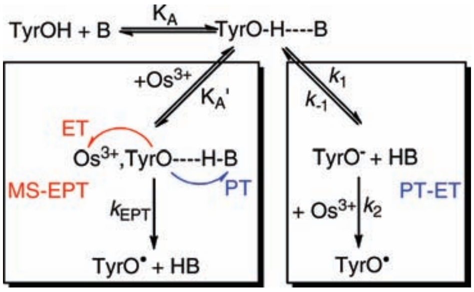

We have also observed electrocatalysis of phenol oxidation at **ITO-Os^{II}** based on the less strongly oxidizing ITO-Os$^{III/II}$ couple with $E°'$ = 0.80 V. Oxidation of TyrOH by Os(bpy)$_3{}^{3+}$ in solution (pH 7) is relatively slow with $k_0(25 \pm 2\ °\text{C}, I = 0.8\ \text{M}) = 1.7 \times 10^2$ M^{-1} s^{-1}.[1] Significant rate enhancements are observed with added buffer bases. They arise from the initial TyrOH---B adduct formation, followed by MS-EPT oxidation with k values ranging from 2.0 × 10^5 [acetate pK_a($^+$HB) = 4.7] to 3.7 × 10^6 M^{-2} s^{-1} (Tris, pK_a = 8.1). MS-EPT is in competition with proton transfer, followed by electron transfer (PT−ET; Scheme 3).[2]

In Figure 3 are shown the cyclic voltammograms of **ITO-Os^{II}** with added citrate (pK_a = 6.4) and Tris (pK_a = 8.1) with and without added TyrOH at a scan rate of 300 mV/s. With added Tris (4.5 mM), significant electrocatalysis is observed. As shown in Figures SI9 and SI10 in the SI, i_p for the surface wave varies with ν and the TyrOH oxidation wave with $\nu^{1/2}$, as found for **ITO-Ru^{II}**. At constant [Tris], E_p for TyrOH oxidation varies with pH from 0.97 V at pH 6.6 ($^+$HB/B = 31.6) to 0.91 V at pH 7.6 ($^+$HB/B = 3.1). The pH dependence is consistent with the predicted pH dependence of the TyrO$^\bullet$/TyrOH couple, $\text{TyrOH} \xrightarrow{-e} \text{TyrO}^\bullet + \text{H}^+$.[3]

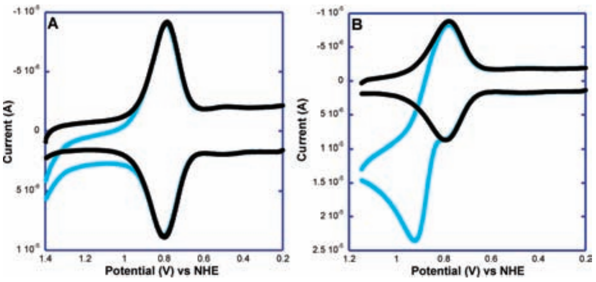

Figure 3. Oxidation of 0.1 mM tyrosine (blue) at **ITO-Os^{II}** [$E_{1/2}$ = 0.8 V vs NHE; $\Gamma/\Gamma_0 = 1$ ($\Gamma_0 = 1.2 \times 10^{-10}$; black) in 0.8 M $LiClO_4$ at 300 mV/s with 50 mM added buffer (10:1 acid/base)]: (A) citrate ($H_3C_6H_5O_7$/$H_2C_6H_5O_7^-$), pH 5.4; (B) Tris [$(HOCH_2)_3CNH_3^+$/$(HOCH_2)_3CNH_2$], pH 7.1.

Scheme 4

$$\mathrm{TyrOH + B \rightleftharpoons TyrOH{-}{-}{-}B}: \mathrm{K_A}$$

$$\mathrm{TyrOH{-}{-}{-}B \longrightarrow TyrO^- + {}^+H\text{-}B}$$

$$\mathrm{ITO\text{-}Os^{2+} \overset{e^-}{\rightleftharpoons} ITO\text{-}Os^{3+}}$$

$$\mathrm{ITO\text{-}Os^{3+} + TyrO^- \longrightarrow ITO\text{-}Os^{2+} + TyrO^{\bullet}}: k_{\mathrm{TyrO-}}$$

$$\mathrm{ITO\text{-}Os^{3+} + TyrOH{-}{-}B \rightleftharpoons ITO\text{-}Os^{3+}{,}TyrOH{-}{-}B}: \mathrm{K_A}'$$

$$\mathrm{ITO\text{-}Os^{3+}{,}TyrOH{-}{-}B \longrightarrow ITO\text{-}Os^{2+} + TyrO^{\bullet} + {}^+HB}: k_{\mathrm{EPT}}$$

$$\mathrm{2TyrO^{\bullet} \longrightarrow (TyrO)_2}$$

Surface electrocatalysis under these conditions presumably occurs by a mechanism analogous to that of Scheme 2 with prior adduct formation, followed by a combination of interfacial MS-EPT and initial proton loss, followed by oxidation of $TyrO^-$ (PT−ET, Scheme 4). Consistent with this conclusion, at fixed pH, i_p for TyrOH oxidation increases linearly with [Tris] (Figure SI11 in the SI). The first-order dependence is consistent with adduct formation, followed by oxidation at the electrode.

Peak current measurements with added buffer in a 10:1 acid/base ratio with pH = pD = 7.1 with added Tris in H_2O and D_2O reveal a H_2O/D_2O KIE of 2.1. For the oxidation of TyrOH by $Os(bpy)_3^{3+}$ in solution with added Tris by the mechanism in Scheme 3, $k_{EPT}K_A(H_2O)/k_{EPT}K_A(D_2O) = 2.3$ and $k_{TyrO^-}K_A(H_2O)/k_{TyrO^-}K_A(D_2O) = 1.3$. This comparison suggests involvement of MS-EPT in the surface reaction.[1,2]

The observations made here are striking in demonstrating the impact of surface-bound electron-transfer relays **ITO-Ru^{II}** and **ITO-Os^{II}** on interfacial electron transfer. They also provide clear evidence for an important role for interfacial EPT at modified surfaces with potentially important implications for analysis and electrocatalysis at derivatized oxide surfaces.

■ ASSOCIATED CONTENT

Ⓢ Supporting Information. Experimental information and characterization of surface-modified electrodes and additional electrochemical analysis including scan-rate-dependent experiments. This material is available free of charge via the Internet at http://pubs.acs.org.

■ AUTHOR INFORMATION

Corresponding Author

*E-mail: tjmeyer@email.unc.edu.

■ ACKNOWLEDGMENT

This work has been supported by the National Science Foundation under Grant CHE-0957215. J.W.J. provided slides of **ITO-Ru^{II}**, and was supported as part of the UNC EFRC: Solar Fuels and Next Generation Photovoltaics, an Energy Frontier Research Center funded by the U.S. Department of Energy, Office of Science, Office of Basic Energy Sciences, under Award DE-SC0001011.

■ REFERENCES

(1) Fecenko, C. J.; Meyer, T. J.; Thorp, H. H. *J. Am. Chem. Soc.* **2006**, *128*, 11020–11021.

(2) Fecenko, C. J.; Thorp, H. H.; Meyer, T. J. *J. Am. Chem. Soc.* **2007**, *129*, 15098–15099.

(3) Costentin, C.; Louault, C.; Robert, M.; Savéant, J. M. *Proc. Natl. Acad. Sci. U.S.A.* **2009**, *106*, 18143–18148.

(4) Jurss, J. W.; Concepcion, J. C.; Norris, M. R.; Templeton, J. L.; Meyer, T. J. *Inorg. Chem.* **2010**, *49*, 3980–3982.

(5) Gillaizeau-Gauthier, I.; Odobel, F.; Alebbi, M.; Argazzi, R.; Costa, E.; Bignozzi, C. A.; Qu, P.; Meyer, G. J. *Inorg. Chem.* **2001**, *40*, 6073–6079.

(6) Hornstein, B. J.; Dattlebaum, D. M.; Schoonover, J. R.; Meyer, T. J. *Inorg. Chem.* **2007**, *46*, 8139–8145.

(7) Meyer, T. J.; Meyer, G. J.; Pfennig, B. W.; Schoonover, J. R.; Timpson, C. J.; Wall, J. F.; Kobusch, C.; Chen, X. H.; Peek, B. M.; Wall, C. G.; Ou, W.; Erickson, B. W.; Bignozzi, C. A. *Inorg. Chem.* **1994**, *33*, 3952.

(8) Bard, A. J.; Faulkner, L. R. *Electrochemical Methods; Fundamentals and Applications*; Wiley: New York, 2001; p 591.

(9) Sjödin, M.; Irebo, T.; Utas, J. E.; Lind, J.; Merényi, G.; Åkermark, B.; Hammarström, L. *J. Am. Chem. Soc.* **2006**, *128*, 13076–13083.

(10) Carra, C.; Iordanova, N.; Hammes-Schiffer, S. *J. Am. Chem. Soc.* **2003**, *125*, 10429–10436.

(11) The ditryosine product has not been characterized and is assumed in the derivation of the rate constants.

(12) Alleman, K. S.; Weber, K.; Creager, S. E. *J. Phys. Chem.* **1996**, *100*, 17050–17058.

(13) Albery, W. J.; Hillman, A. R. *J. Electroanal. Chem.* **1984**, *170*, 27–49.

(14) Andrieux, C. P.; Saveant, J. M. In *Techniques of Chemistry: Molecular Design of Electrode Surfaces*; Murray, R. W., Ed.; Wiley: New York, 1992; Vol. 22; pp 207−270.

(15) Young, R. C.; Keene, F. R.; Meyer, T. J. *J. Am. Chem. Soc.* **1977**, *99*, 2468–2473.

(16) Nakagawa, T.; Beasley, C. A.; Murray, R. W. *J. Phys. Chem. C* **2009**, *113*, 12958–12961.

(17) The shift in E_p to 1.24 V in 10^{-3} M $HClO_4$ and a dilute 1×10^{-5} M citrate ($H_3C_6H_5O_7$/$H_2C_6H_5O_7^-$) buffer from 1.31 V in 0.1 M $HClO_4$ (Figure SI7 in the SI) provides evidence for the participation of surface phosphonate groups with $pK_a \sim 1.5$ acting as an EPT acceptor base.[18]

(18) Jurss, J. W.; Gagliardi, C. J.; Meyer, T. J. **2011**, in preparation.

(19) Carra, C.; Iordanova, N.; Hammes-Schiffer, S. *J. Am. Chem. Soc.* **2003**, *125*, 10429–10436.

(20) Dixon, W. T.; Murphy, D. *J. Chem. Soc., Faraday Trans.* **1975**, *72*, 1221–1230.

(21) Huynh, M. H.; Meyer, T. J. *Chem. Rev.* **2007**, *107*, 5004–5064.